Organic & Biomolecular Chemistry

Accepted Manuscript

ROYAL SOCIETY OF CHEMISTRY

www.rsc.org/obc

Organic & Bimolecular Chemistry

RSCPublishing

ARTICLE

Hydroxyl Radical Induced Oxidation of Theophylline in Water: A Kinetic and Mechanistic Study

Cite this: DOI: 10.1039/xoxxoooooox

M. M. Sunil Paul,[a] U. K. Aravind,[b] G. Pramod,[c] A. Saha,[d] and C. T. Aravindakumar[a,e]*

Received ooth January 2012,
Accepted ooth January 2012

DOI: 10.1039/xoxxoooooox

www.rsc.org/

Oxidative destruction and mineralization of emerging organic pollutants by hydroxyl radical ($^{\bullet}$OH) is a well established area of research. The possibility of generating hazardous by-products in the case of $^{\bullet}$OH reaction demands extensive investigations on the degradation mechanism. A combination of pulse radiolysis and steady state photolysis (H_2O_2/UV photolysis) followed by high resolution mass spectrometric (HRMS) analysis have been employed to explicate the kinetic and mechanistic features of the destruction of theophylline, a model pharmaceutical compound and an identified pollutant, by $^{\bullet}$OH in the present study. The oxidative destruction of this molecule, for intermediate product studies, was initially achieved by H_2O_2/UV photolysis. The transient absorption spectrum corresponding to the reaction of $^{\bullet}$OH with theophylline at pH 6, primarily caused by the generation of (T8-OH)$^{\bullet}$, was characterised by an absorption band at 330 nm (k_2 = (8.22 ± 0.03) × 10^9 dm^3 mol^{-1} s^{-1}). A significantly different spectrum (λ_{max}: 340 nm) was observed at highly alkaline pH (10.2) due to the deprotonation of this radical (pKa ~ 10.0). Specific one electron oxidants such as sulphate radical anion ($SO_4^{\bullet-}$) and azide radical ($N_3^{\bullet}$) produces the deprotonated form (T(-H)$^{\bullet}$) of the radical cation ($T^{\bullet+}$) of theophylline (pKa 3.1) with a k_2 values of (7.51 ± 0.04) × 10^9 dm^3 mol^{-1} s^{-1} and (7.61 ± 0.02) × 10^9 dm^3 mol^{-1} s^{-1} respectively. Conversely, oxide radical ($O^{\bullet-}$) reacts with theophylline *via* a hydrogen abstraction protocol with a rather slow k_2 value of (1.95 ± 0.02) × 10^9 dm^3 mol^{-1} s^{-1}. The transient spectral studies were complemented by the end product profile acquired by HRMS analysis. Various transformation products of theophylline induced by $^{\bullet}$OH were identified by this technique which include derivatives of uric acids (**i, iv** & **v**) and xanthines (**ii**, **iii** & **vi**). Further breakdown of the early formed product due to $^{\bullet}$OH attack leads to ring opened compounds (**ix**-**xiv**). The kinetic and mechanistic data furnished in the present study serves as a basic frame work for the construction of $^{\bullet}$OH induced water treatment systems as well as to understand the biological implications of compounds of this kind.

1. Introduction

Hydroxyl radicals ($^{\bullet}$OH) are the key species responsible for the oxidative destruction of environmental pollutants in many Advanced Oxidation Processes (AOPs) such as TiO_2 photocatalysis, H_2O_2/UV photolysis, sonolysis, γ-radiolysis etc[1-7] and many biological processes including DNA damage, mutation and ageing.[8-16] The $^{\bullet}$OH induced destruction of emerging organic pollutants is widely experimented[1-4, 7, 17, 18] since the presence of pharmaceutically active compounds in the aquatic environment became an emerging environmental issue.[19-22] Pulse radiolysis studies reveals that $^{\bullet}$OH reacts with a large number of organic molecules with a nearly diffusion controlled rate.[5,6,12,15,23,24] Furthermore, the ability to achieve complete mineralization[2,6] makes techniques of these kinds in to most acceptable and environmental friendly.

Conversely, recent studies using high resolution mass spectrometric (HRMS) techniques demonstrated that the formation of aromatic intermediates (that are likely toxic) as a result of $^{\bullet}$OH attack is viable in the case of a number of organic compounds.[5, 6, 17, 18] This impacts serious health problems on targeted organisms because of their potential biological activities. The kinetic and mechanistic investigation of the reaction mechanism, including the identification of the transient intermediate products as well as the stable transformation products, is thus very important in the case of any $^{\bullet}$OH mediated destruction protocol prior to its implementation in real system.

Theophylline (trade name: Deriphyllin), an extensively used drug for the therapy of different respiratory diseases such as

chronic obstructive pulmonary disease (COPD), asthma etc,[25-27] is taken as a model compound for this study. It is naturally found in a variety of products such as cocoa beans (~ 3 mg/g), green tea (~ 0.5 g/kg), coffee, chocolate and cola beverages in variable amount.[25-27] It is reported as a metabolite of caffeine[28] and a number of naturally occurring alkaloids.[29] It enhances the anti-inflammatory effect of steroids by increasing the histone deacetylases (HDAC) activity.[30] Theophylline is moderately toxic to mammals (LD50 > 200 mg/kg) such as mice, rabbits, rats etc[31] and exhibits a negative (Log P at pH 7 and 20°C is -0.02) octane-water partition coefficient.[32] It is reported that higher doses of theophylline (> 20 µg/ml) cause serious health problems (such as cardiac arrest, arrhythmias and hypotension) in humans.[25-27, 33] A recent report by Antoniou and co-workers demonstrated that the toxicity of theophylline increases (around double) when it is administrated with Ciprofloxacin, a widely used fluoroquinolone antibiotic.[34] Furthermore, presence of this compound in the aquatic environment is recently reported.[21, 22] Bioaccumulation and specific biological activities of the pharmaceutically active compounds like theophylline makes them harmful to the targeted organisms especially in the case of aquatic environment.[21,22] The studies on the removal/degradation of this compound from the aqueous medium is consequently a very relevant topic of investigation.

The destruction of this compound by one of the AOP techniques (photocatalysis) is recently reported.[35] However, detailed information on the kinetic and mechanistic aspects of its reaction with $^{\bullet}OH$ is very limited.[36] An in-depth understanding of the kinetic and mechanistic aspects of the $^{\bullet}OH$ reaction of this compound is thus very necessary for the proper application of AOP techniques for the removal of this compound from water. A systematic investigation of the reaction of theophylline in aqueous medium using photolytically produced hydroxyl radical (H_2O_2/UV) is carried out in the present study. The kinetics of this reaction and the formation of possible transient intermediate radicals has been probed using pulse radiolysis technique. In order to obtain more insights in to the underlying reaction mechanism, the end products formed during the reaction were evaluated using the state-of-the-art mass spectrometric method. Additionally, a comparison of $^{\bullet}OH$ reaction of this compound, on the transient spectra and product profile, with some of the more specific radicals ($SO_4^{\bullet-}$, $N_3^{\bullet}$ and $O^{\bullet-}$) was also carried out. An in-depth mechanistic understanding of the reaction of this compound with oxidizing radicals is very valuable in the case of Advanced Oxidation Technologies as well as in biological system mainly due to the anti-oxidant properties of methylxanthines[28,36] and its structural similarities with purine bases.

2. Materials and Methods

Theophylline (1,3-Dimethyl-3,9-dihydro-1H-purine-2,6-dione, CAS No. 58-55-9) was purchased from Sigma Aldrich and was used as received. Potassium persulfate, 2-methyl-2-propanol, sodium azide and sodium hydroxide were obtained from Fischer scientific. High purity N_2O and Ar gas was used for pulse radiolysis experiments. HPLC and LC-MS grade solvents were used for the HPLC and LC-Q-TOF-MS analysis respectively.

2.1. Steady state photolysis

Steady state photolysis experiments in presence of hydrogen peroxide (H_2O_2/UV photolysis) was carried out on a photo reactor supplied by Scientific Aids & Instruments Corporation (SAIC, Chennai). The reactor utilizes a 125 W medium pressure deuterium lamp as the light source, which is kept in a quartz vessel. The lamp emits continuous light spectrum between 185 nm to 400 nm region. All the experiments were carried out at near natural pH (~ 6) and room temperature.

2.2. HPLC analysis

The variation in the concentration of theophylline after H_2O_2/UV photolysis was monitored by using a Shimadzu LC-20AD Prominence Liquid Chromatography system coupled with Diode Array Detector (at 270 nm). An isocratic elution of methanol and water (25:75) at a flow rate of 0.8 mL min^{-1} against an enable C18G column (250 mm × 4.6 mm × 5 µm) was used as mobile phase.

2.3. LC-Q-TOF-MS analysis

The stable transformation products of theophylline formed during the reaction of $^{\bullet}OH$ were analyzed on a Waters Acquity H class UPLC system coupled with a Waters Xevo G2 Quadrapole – Time-of-Flight (Q-TOF) high resolution mass spectrometer (HRMS) in which electrospray (ESI) technique was used for the ionization. The samples were introduced into the mass spectrometer through a BEH C18 column (50 mm × 2.1 mm × 1.7 µm). A gradient elution of methanol and Water (0.3 mL min^{-1}) was used as the mobile phase. All the spectra were recorded in both positive and negative ionization modes between mass-to-charge (m/z) ranges of 50 – 600 Da.

2.4. Pulse radiolysis experiments

Time resolved transient spectroscopic studies of the intermediates were carried out on a 7 MeV linear electron accelerator (AS & E, USA) connected to an optical absorption detection system (Luzchem, Canada) which consists of a Cermax parallel lamp (175 W), a monochromator and Hamamastu photomultiplier (R-7400U-04). The dose per pulse of the electron beam was determined by KSCN dosimetry as per reported procedure and was found to be around 16 Gy per 100 ns pulse[37]. The transient species generated as a result of pulse irradiation was monitored by time resolved UV-Visible spectroscopy. All other details of the accelerator and detection system have been published elsewhere.[38] Formation of primary radicals along with ionic and molecular species by radiolysis of water and the creation of an oxidative environment by removing reducing species using N_2O gas are given in equation 1 and 2.[23]

$$H_2O \ \text{/\\/\\/\\->} \ ^{\bullet}OH\ (0.28),\ H^{\bullet}\ (0.06),\ e_{aq}^{-}\ (0.27),\ H^{+}\ (0.27),\ H_2\ (0.05),\ H_2O_2\ (0.07) \quad (1)$$

$$e_{aq}^{-} + N_2O + H_2O \rightarrow N_2 + {}^{\bullet}OH + {}^{-}OH \quad (2)$$

The values given in the parenthesis are called G-values which represent the number of species formed per 100 eV of the incident radiation.[18, 23]

3. Results and Discussion

3.1. Steady state degradation studies

Preliminary experiments were performed for evaluating the efficiency of $^{\bullet}OH$ mediated destruction of this drug. The initial concentration of theophylline for these experiments were fixed as 1×10^{-5} mol dm^{-3} in order to have a workable sensitivity for the HPLC-DAD system, though it is considerably higher than the reported concentration of pharmaceutical compounds in

water.[21, 22] The photo-irradiation in the presence of H_2O_2 results a complete disappearance of theophylline within 8 min. Figure 1 shows the degradation profile of this compound as a function of irradiation time. At this timescale, the destruction of theophylline by the direct effect of UV radiation is not significant (data not shown).

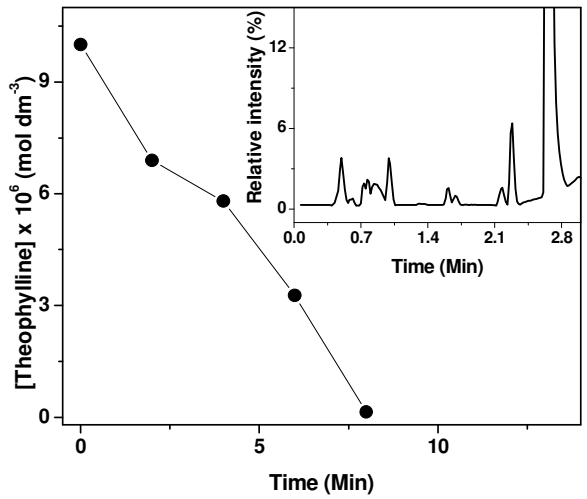

Figure 1. Photo-degradation profile of theophylline in the presence of H_2O_2 as a function of time. $[Theophylline]_0 = 1 \times 10^{-5}$ mol dm^{-3}; $[H_2O_2]_0 = 5 \times 10^{-5}$ mol dm^{-3}. (Inset) Total Ion Chromatogram of theophylline after H_2O_2/UV photolysis. ($[Theophylline]_0 = 1 \times 10^{-5}$ mol dm^{-3}; Transformation of theophylline = 37.5%).

It is well-known that photolysis of H_2O_2 yields $^{\bullet}OH$ (equation 3).[23] The entire degradation is thus attributed to the oxidation reaction initiated by $^{\bullet}OH$.

$$H_2O_2 + h\nu \rightarrow 2^{\bullet}OH \qquad (3)$$

The efficient destruction of this compound induced by $^{\bullet}OH$ is very promising especially for the remediation of this pollutant from aquatic environment. On the other hand, this kind of degradation may not lead to a complete mineralisation of the pollutants. It may also result a number of intermediate products which may be hazardous too. Considering these possibilities, it is proposed that a thorough understanding on the kinetic and mechanistic aspects of the reaction leading to the destruction of this compound is very important and should be evaluated.

3.2. Product Analysis

One of the convenient ways of end product profiling is the use of a high resolution mass spectrometric (HRMS) method such as LC-Q-TOF-MS which provides the accurate masses of each compound. Another advantage of LC-Q-TOF-MS is the ability to analyze highly complex samples without any pre-purification. LC-Q-TOF-MS analyses were carried out on a number of photo irradiated samples in which nearly 20 - 60% of the parent compound was transformed into different products. To enhance the possibility of detecting minor products that are expected to be in very in low concentrations, an initial concentration of 1×10^{-4} mol dm^{-3} theophylline is employed for product studies. The Total Ion Chromatogram (TIC) of theophylline after 6 min of UV irradiation in the presence of H_2O_2 is shown in figure 1.

The peak with m/z 181 (obs. Mass 181.0727; calcd. for $C_7H_9N_4O_2$ is 181.0726) in positive mode (ESI+) and 179 (obs. Mass 179.0565; calcd. for $C_7H_7N_4O_2$ is 179.0569) in negative mode (ESI-) represents the parent molecule (data not shown). All other peaks in the TIC stand for various oxidation products of theophylline. To gain further structural features of various peaks in the TIC, MS/MS studies were carried out. The primary products formed during the reaction of theophylline with $^{\bullet}OH$ comprise a hydroxylation product (**i**) and two isomeric demethylation products (**ii & iii**). Compound **i** (1,3-dimethyluric acid), the major product of this reaction, was characterized by an intense peak at m/z 197 (obs. Mass 197.0675; calcd. for $C_7H_9N_4O_3$ 197.0675) in ESI+ and 195 (obs. Mass 195.0510; calcd. for $C_7H_7N_4O_3$ 195.0518) in ESI-. The demethylation products, 1-methylxanthine (**ii**) and 3-methylxanthine (**iii**), show peaks at m/z 167 (obs. Mass 167.0567; calcd. for $C_6H_7N_4O_2$ 167.0569) in ESI+ and 165 (obs. Mass 165.0412; calcd. for $C_6H_5N_4O_2$ 165.0413) in ESI-. The substantial difference in the MS/MS spectra (figure S1 and S2, Supplementary information) permits the identification of **iii** and **iv** using tandem mass spectrometry. Further transformation of the primary products results isomeric uric acids like 1-methyluric acid (**iv**), 3-methyluric acid (**v**) or xanthine (**vi**). The uric acids (**iv** and **v**) shows peaks at m/z 183 (obs. Mass 183.0518; calcd. for $C_6H_7N_4O_3$ 183.0518) in ESI+ and 181 (obs. Mass 181.0360; calcd. for $C_6H_5N_4O_3$ 181.0362) in ESI- while the mass spectra of xanthine (**vi**) exhibits an intense peak at m/z 153 (obs. Mass 153.0410; calcd. for $C_5H_5N_4O_2$ 153.0413) in ESI+ and 151 (obs. Mass 151.0254; calcd. for $C_5H_3N_4O_2$ 151.0256) in ESI-. Compounds **i–vi** is previously accounted as microbial metabolites of theophylline.[39] The probable mechanism leading to the formations of these compounds are briefly discussed in section 3.4. In addition to these products (i-vi), eight more transformation products (**vii-xiv**) have been identified. Most of these compounds are likely originated by the opening of the imidazole ring of theophylline by $^{\bullet}OH$. The entire list of transformation products, with molecular weight and elemental composition, identified by LC-Q-TOF-MS analysis is given in table 1. The proposed chemical structures of the identified products are presented in Scheme 2. The mass spectra and MS/MS patterns of the transformation products of theophylline are given in the supplementary information (Figure S1-S16).

Table 1. List of transformation products identified by LC-Q-TOF-MS analysis

Sl. No.	Product	Mol. Wt.	Elemental composition
i	1,3-dimethyluric acid	196.16	$C_7H_8N_4O_3$
ii	1-methylxanthine	166.14	$C_6H_6N_4O_2$
iii	3-methylxanthine	166.14	$C_6H_6N_4O_2$
iv	1-methyluric acid	182.14	$C_6H_6N_4O_3$
v	3-methyluric acid	182.14	$C_6H_6N_4O_3$
vi	Xanthine	152.11	$C_5H_4N_4O_2$
vii	1/3-methyl tetrahydro-1H-purine-2,6-dione	168.15	$C_6H_8N_4O_2$
viii	8-hydroxy-1/3-methyl-	184.15	$C_6H_8N_4O_3$

	3,7,8,9-tetrahydro-1H-purine-2,6-dione		
ix	5/6-amino derivative of 5/6-hydroxy-1,3-dimethylpyrimidine-2,4(1H,3H)-dione	171.15	$C_6H_9N_3O_3$
x	5/6-amino derivative of 1/3-methylpyrimidine-2,4(1H,3H)-dione	141.13	$C_5H_7N_3O_2$
xi	5/6-aminopyrimidine-2,4(1H,3H)-dione	127.10	$C_4H_5N_3O_2$
xii	5/6-amino derivative of 5/6-hydroxydihydropyrimidine-2,4(1H,3H)-dione	145.12	$C_4H_7N_3O_3$
xiii	1/3-methylpyrimidine-2,4(1H,3H)-dione	126.11	$C_5H_6N_2O_2$
xiv	5,6-diaminopyrimidine-2,4(1H,3H)-dione	142.12	$C_4H_6N_4O_2$

3.3. Pulse radiolysis studies

In order to obtain more insight into the kinetic and mechanistic aspects of a reaction, the information concerning the short lived intermediates (i.e., initial stages of reaction) is of utmost importance. Pulse radiolysis is the ultimate technique for monitoring the short lived transient species in a nano/micro second time scale.[15] The combination pulse radiolysis and mass spectrometric techniques are proven as the ideal methodology for obtaining valuable mechanistic insights.[5,6,17] The pKa value of theophylline was initially determined by plotting the dependence of absorbance at 272 nm (λ_{max} of theophylline) against pH of the solution (figure 2). Theophylline thus exhibits two distinct pKa (figure 2); one at 3.3 corresponding to the protonation of NH group and another at 9.8 corresponding to the deproptonation of amino group.

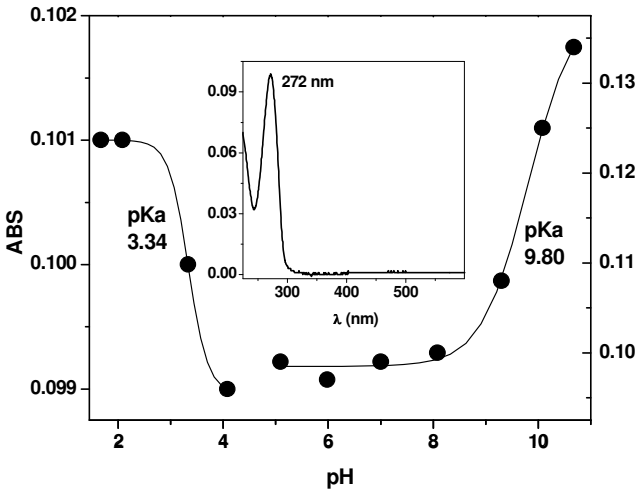

Figure 2. Plot of pH vs absorbance at 272 nm. (Inset) UV-Vis Spectrum of theophylline.

3.3.1. Reaction with hydroxyl radical

Pulse radiolysis of N_2O saturated solution of theophylline at pH 5.9 yielded a transient absorption spectrum having a sharp absorption maximum at 330 nm and a broad absorption around 500 nm (figure 3). The absorption band at 500 nm completely decays within 100 μs with a first order rate constant of 4.91×10^4 s^{-1}. Conversely the absorption band at 330 nm shows a slow decay (figure 3). The bimolecular rate constant corresponding to the reaction of theophylline with hydroxyl radical was determined by following the growth of the transient at the 330 nm within a concentration range of (0.5-1) $\times 10^{-4}$ mol dm^{-3}. A rate constant of $(8.22 \pm 0.03) \times 10^9$ dm^3 mol^{-1} s^{-1} is obtained for this reaction (figure 4).

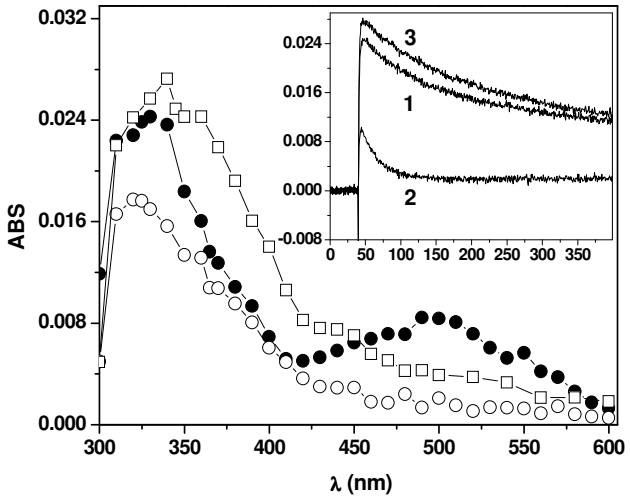

Figure 3. Transient absorption spectrum recorded during the reaction of $^{\bullet}OH$ with theophylline (1×10^{-4} mol dm^{-3}) at pH 5.9 after (●) 10 and (○) 100 μs and at pH 10.2 (□) after 10 μs of the pulse. (Inset) Decay traces at 1) 330 nm (pH 5.9), 2) 500 nm (pH 5.9) and 3) 340 nm (pH 10.2).

Alternatively, the transient absorption spectrum at pH 10.2 (above pKa) shows a red shift (λ_{max}: 340 nm; k_2: $(7.11 \pm 0.07) \times 10^9$ dm^3 mol^{-1} s^{-1}) in the UV region lacking any significant absorption in the visible region (figure 3).

3.3.2. Reaction with oxide radical.

The oxide radical anion ($O^{\bullet-}$) predominantly undergoes one electron transfer and/or hydrogen abstraction reactions.[23] A comparison of the intermediate spectra from this reaction would help in the identification of the intermediate species from $^{\bullet}OH$ reaction. The transient absorption spectrum obtained from the reaction of $O^{\bullet-}$ (at pH > 13) is characterized by two absorption bands at 320 nm and 350 nm (figure 4) without having any noteworthy change in the decay profile (Figure S17, supplementary information). At pH > 13, more than 90% of the hydroxyl radicals are converted into $O^{\bullet-}$ with a pKa value of 11.9 according to the following equation.

$$^{\bullet}OH + {}^{-}OH \leftrightarrow O^{\bullet-} + H_2O \qquad (4)$$

The calculated bimolecular rate constant for the reaction of $O^{\bullet-}$ with theophylline from the formation kinetics (figure 4) at 350 nm is $(1.95 \pm 0.02) \times 10^9$ dm^3 mol^{-1} s^{-1}.

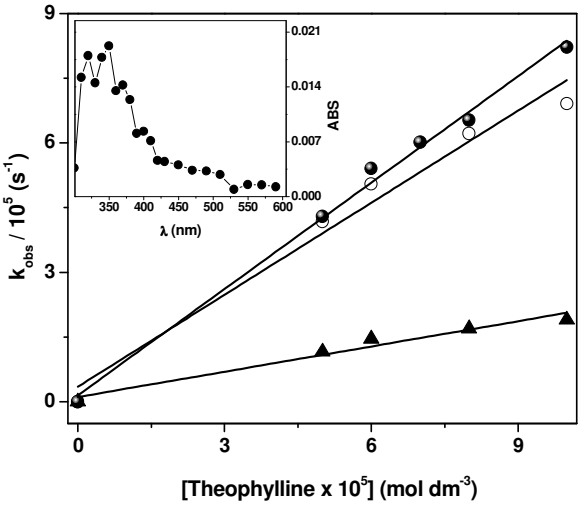

Figure 4. Plot of k_{obs} against [Theophylline] in the case of the reaction of $^{\bullet}OH$ at pH (●) 5.9 (330 nm), (□) 10.2 (340 nm) and (▲) $O^{\bullet-}$ (350 nm). (Inset) Transient absorption spectrum recorded during the reaction of $O^{\bullet-}$ with theophylline (1×10^{-4} mol dm^{-3}) after 20 μs of the pulse.

3.3.3. Reaction with specific one electron oxidants

Being very selective in their reactions, sulfate radical anion ($SO_4^{\bullet-}$) and azide radical ($N_3^{\bullet}$) are ideal for evaluating the contribution of electron transfer reactions in the case of $^{\bullet}OH$ reaction. Generation of $SO_4^{\bullet-}$ and $N_3^{\bullet}$ by pulse radiolysis is exemplified in reactions 5 -7.[40-42]

$$(CH_3)_3COH + {}^{\bullet}OH \rightarrow {}^{\bullet}CH_2(CH_3)_2COH + H_2O \quad (5)$$
$$S_2O_8^{2-} + e_{aq}^- \rightarrow SO_4^{\bullet-} + SO_4^{2-} \quad (6)$$
$$N_3^- + {}^{\bullet}OH \rightarrow N_3^{\bullet} + {}^-OH \quad (7)$$

Reaction of $SO_4^{\bullet-}$ at pH 6.0 yielded a transient absorption spectrum having a broad absorption band around 320 - 380 nm region (Figure 5). A bimolecular rate constant of (7.51 ± 0.04) × 10^9 dm^3 mol^{-1} s^{-1} is obtained for this reaction (Figure 5).

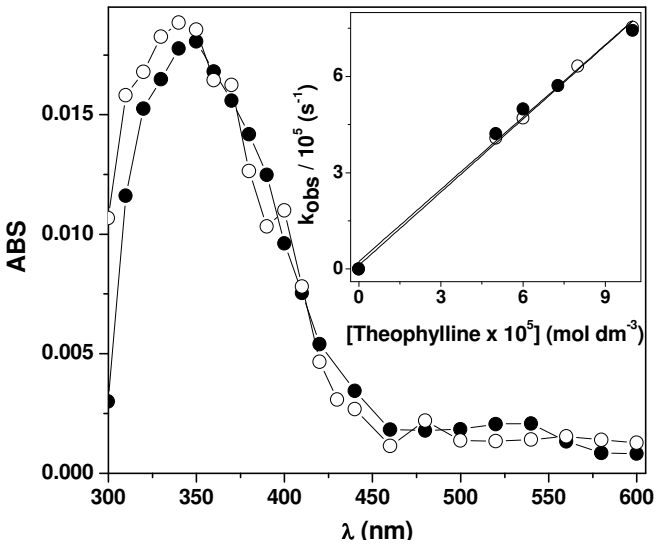

Figure 5. Transient absorption spectrum of theophylline (1×10^{-4} mol dm^{-3}) recorded during its reaction with $SO_4^{\bullet-}$ after (●) 7 μs (pH 6.0) and with $N_3^{\bullet}$ after (O) 6 μs (pH 6.1). (Inset) Plot of k_{obs} against [Theophylline] in the case of reaction of (●) $SO_4^{\bullet-}$ (350 nm) and (o) $N_3^{\bullet-}$ (340 nm).

The reaction of sulfate radical with theophylline at a more basic pH (9.3) also shows an absorption band at the same region (data not shown) though the bimolecular rate constant (k_2 = (5.37 ± 0.03) × 10^9 dm^3 mol^{-1} s^{-1}) obtained in this case is somewhat lower.

Transient absorption spectra having complementary nature were obtained in the case of reaction of $N_3^{\bullet}$ at pH 6.1 (figure 5), 4.0 and 9.5 (data not shown). The bimolecular rate constant obtained at pH 6.1 (k_2 = (7.61 ± 0.02) × 10^9 dm^3 mol^{-1} s^{-1}) and 9.6 (k_2 = (8.42 ± 0.06) × 10^9 dm^3 mol^{-1} s^{-1}) are very similar. However, the rate constant value obtained at pH 4 (k_2 = (4.05 ± 0.02) × 10^9 dm^3 mol^{-1} s^{-1}) is reduced to nearly half. It is noteworthy to mention the fast decay of transient, with a first order rate constant (k_{obs}) of 3.0 × 10^4 s^{-1}, at pH 6 though a moderately slow decay is observed in the case of reaction of $SO_4^{\bullet-}$. The substantial variation in the decay profile of transient in the case of $SO_4^{\bullet-}$ is accounted by interference caused by absorption of $SO_4^{\bullet-}$ from the UV region. It is also worth to mention the similarities of both spectra ($SO_4^{\bullet-}$ and $N_3^{\bullet}$) at higher timescales (less interference of $SO_4^{\bullet-}$; Figure S18, Supplementary information). The spectral and kinetic parameter of different radicals on its reaction with theophylline is summarized in table S1 of supplementary information.

As a consequence of the structural similarities of theophylline with purine, it is presumed to go through a similar reaction protocol with $^{\bullet}OH$. Recent works of Chatgilialoglu and co-workers recommended that the main site of hydroxyl radical attack in the base part of guanosine and deoxyguanosine moiety is the exocyclic amino group (~ 65%) whereas the hydroxylation at C8 (~ 17%) position plays only a minor role.[9, 10] The lack of amino group in theophylline results the primary reaction of hydroxyl radical at carbon 8 to form corresponding hydroxyl radical adduct of the form $(T8\text{-}OH)^{\bullet}$ represented as in scheme 1. The analogous stable product, 1,3-dimethyluric acid (**i**), identified in our end product studies further supports this assignment. The generation of a similar kind of radical is formerly reported in the case of oxidation of caffeine.[43]

The C8-OH adduct of (deoxy) guanosine generally undergoes i) opening of the imidazole ring (yields compounds like 2,6-diamino-4-hydroxy-5-formamidopyrimidine, commonly referred as FapyG)[10] and ii) bimolecular transformation to 8-oxoguanine.[10] Product studies using LC-Q-TOF-MS perceives analogues compounds corresponding to these reactions suggesting the feasibility of both processes in the present case. When the samples after pulse irradiation were subjected to end product studies, demethylated products like 1 and 3-methylxanthine (**ii** and **iii**), were detected. Demethylation is supposed to begin with hydrogen abstraction (see section 3.4.2), the contribution of radical(s) generated by hydrogen abstraction from the methyl side chains of theophylline is expected in the transient spectrum. Therefore, it is proposed that, the experimental spectrum observed in the case of reaction of $^{\bullet}OH$ with theophylline has a contribution from the radicals **b** and **c** in addition to the primary radical **a**. The evidence for the absorbance of the radicals **b** and **c** came from the interpretation of the transient spectrum resulting from the reaction of $O^{\bullet-}$, which is known to generate hydrogen abstracted species selectively[23] (discussion followed). The exact contribution of

these individual radicals is difficult to predict. However, it is assumed that the main absorbing species is the radical **a** since it is well known that $^{\bullet}$OH predominantly undergoes addition with similar compounds and such adduct radicals exhibit characteristic absorption bands at this region.[10,12,15,18] On the other hand, the slow decay observed at 330 nm compared to 500 nm at pH 6 (figure 3) could be due to the interference of the radicals **b** and **c**. It is also predicted that the weak absorption around 500 nm is the contribution of radical **a** since there is no information on the formation of other OH adduct radicals as demonstrated in our LC-Q-TOF-MS results.

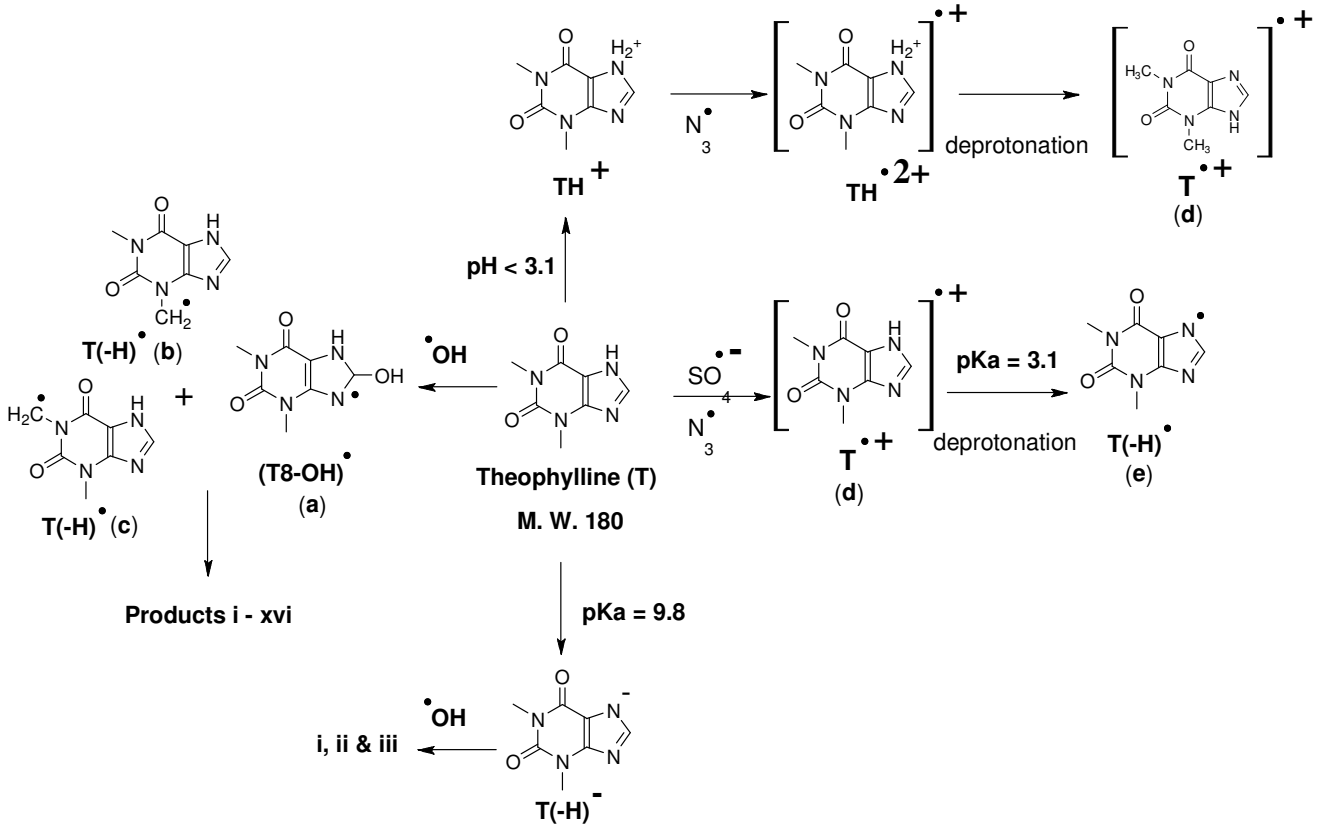

Scheme 1. Proposed mechanism of the reaction $^{\bullet}$OH, $SO_4^{\bullet-}$, $N_3^{\bullet}$ and $O^{\bullet-}$ with theophylline.

At higher alkaline pH, theophylline exists as its deprotonated form represented as $(T\text{-}H)^-$ (pKa ~ 9.8) in scheme 1. The transient absorption spectrum recorded in the case of reaction of $^{\bullet}$OH with theophylline at pH 10.2 was different from that of pH 6.0 by a red shift in the λ_{max} and a higher absorbance value at UV region (figure 3). A similar shift in λ_{max} and absorbance values was also noticed in the ground state absorption spectrum of theophylline (Figure S19, Supplementary information). The product profile obtained from the high resolution mass spectrometer is nearly similar to that of pH 6.0 apart from the lack of ring-opened products like **ix**. Since 1,3-dimethyluric acid is also detected at this pH, the addition of $^{\bullet}$OH at carbon 8 is likely responsible for the transient absorption. The plot of absorbance corresponding to this transient (monitored at 330 nm) as a function of pH gave a clear pKa curve having an inflection point around pH 10.0 (figure S20, Supplementary data). Differences in the transient spectrum of theophylline on its reaction with $^{\bullet}$OH at pH 10.2 is thus explained on the basis of the deprotonation of the $(T8\text{-}OH)^{\bullet}$. A similar mechanism is previously reported in the case of a series of pyrimidine derivatives.[12] The lack of product **ix** at pH 10.2 indicates the less feasibility of ring opening reaction of $(T8\text{-}OH)^{\bullet}$ above the pKa of theophylline.

It is well-known that one electron oxidants such as $N_3^{\bullet}$ and $SO_4^{\bullet-}$ results radical cation on its reaction with purines and other aromatic systems.[15,44] Because of the high bronsted acidity, the radical cation thus formed either reacts with H_2O/OH^- (depends on pH) and yields a hydroxyl radical adduct or deprotonated in to a neutral radical.[15,45] If former is the case, the corresponding transient spectra should match with that of the one obtained with $^{\bullet}$OH reaction. However, it is not observed in the present case (figure 3 and 5). In addition, the end product studies on the photo-irradiated samples in the presence of $K_2S_2O_8$ (generates $SO_4^{\bullet-}$ in the medium)[45] did not provide any evidence for the formation of 1,3-dimethyluric acid (see section 3.4.2). The remaining possibility is the deprotonation of radical cation in to a neutral radical represented as $T(\text{-}H)^{\bullet}$ (**e**). Previous studies by santos et al in the case of one-electron oxidized methylxanthines recommended the formation of a N_7 deprotonated neutral radical with significant stability.[46]

The studies on the fate of radical cations are pertinent in biological systems because of its involvement in diseases like cancer.[47,48] To gain more mechanistic aspects of the deprotonation of radical cation, the absorbance of the transient at 340 nm obtained in the case of reaction of theophylline with $N_3^{\bullet}$ were monitored as a function of pH. The result is shown in

figure 6. The inflection point at pH 3.1 obtained by this experiment suggests the existence of radical cation, without deprotonation, only below pH 3.1. The determined pKa value of theophylline radical cation is very close to that of guanine.[15, 44]

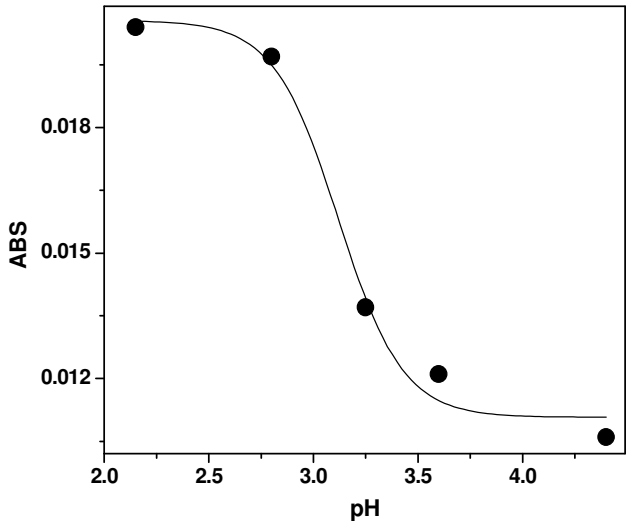

Figure 6. Plot of absorbance of transient at 340 nm against pH in the case of reaction of $N_3^{\bullet -}$

Another explanation for the existence of radical cation at highly acidic pH is that the protonated form of theophylline (pKa ~ 3.3), represented as TH^+, undergo one electron oxidation with $N_3^{\bullet}$ to form a $TH^{\bullet 2+}$ (**f**). The $TH^{\bullet 2+}$ is expected to be highly unstable and instantly releases a proton to yield theophylline radical cation ($T^{\bullet +}$). Hence, the broad absorption band obtained between 320-380 nm in the case of reaction of $N_3^{\bullet}$ and $SO_4^{\bullet -}$ (figure 5) at neutral and basic pH is assigned to the N_7 deprotonated neutral radical $T(-H)^{\bullet}$ (Scheme 1).

One electron transfer and/or hydrogen abstraction reactions are accounted as the primary route of the reaction of $O^{\bullet -}$ with aromatic compounds.[23] If electron abstraction is the case, an N_7 deprotonated radical (**e**) will be the possible intermediate. Since the reaction of theophylline with specific one electron oxidants, that is $SO_4^{\bullet -}$ and $N_3^{\bullet}$, also generates the same radical, a similar spectrum is presumed. However, this is not observed in the present case (figure 4 and 5). The only remaining possibility is the abstraction of a hydrogen atom from either of the methyl side chains of theophylline to form another carbon centered $T(-H)^{\bullet}$ radical (**b** or **c**). Hence, the absorption bands obtained in the present case is likely due to the formation of radicals **b** or/and **c**. It is also worth to mention the low bimolecular rate constant ($k_2 = (1.95 \pm 0.02) \times 10^9$ dm^3 mol^{-1} s^{-1}) determined for this reaction (k_2 values corresponding to the hydrogen abstraction reactions are usually low).[23]

3.4. Reaction Mechanism

The various transformation products corresponding to the reaction of $^{\bullet}$OH with theophylline are already discussed in section 3.2. The transformation pathways of theophylline on its reaction with $^{\bullet}$OH are classified in to three stages (stage 1-3) and are described in scheme 2. Stage 1 explains the formation of primary products of theophylline (scheme 3 and 4) whereas stage 2 and 3 explains further transformation of the primary products. The mechanism of formation the primary products induced by $^{\bullet}$OH are separately discussed in scheme 3-4.

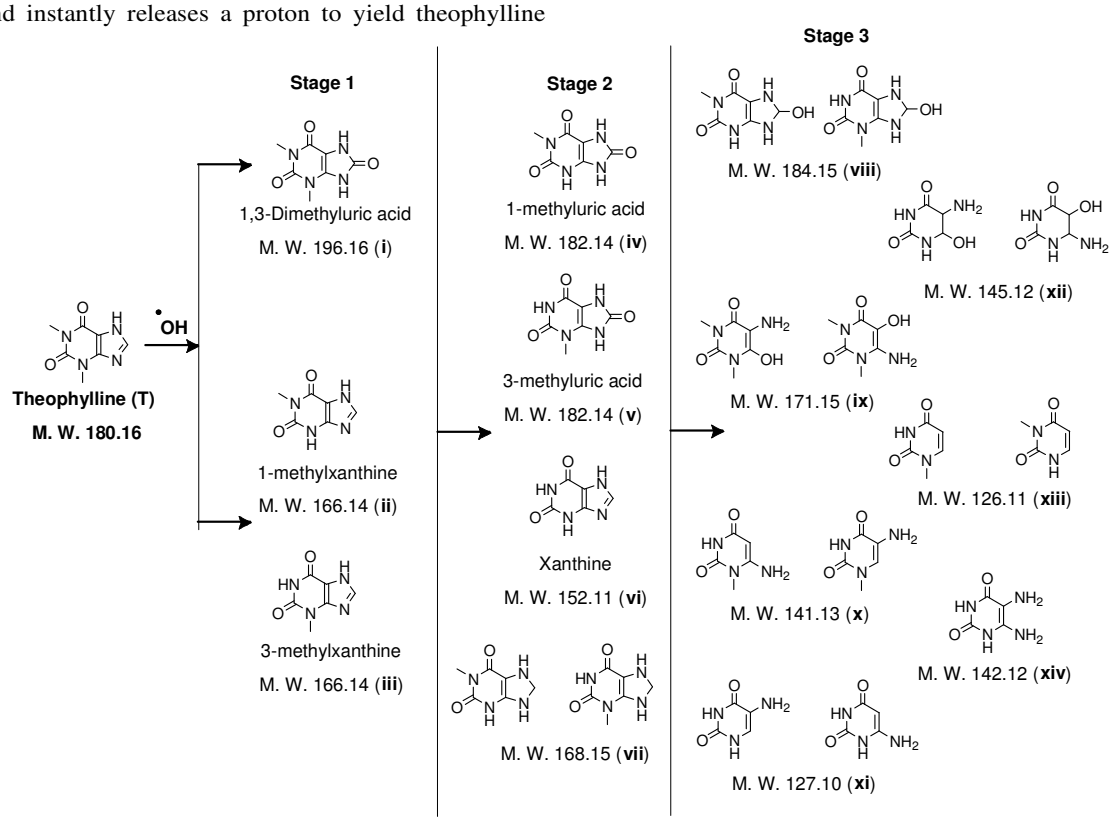

Scheme 2. Proposed degradation pathways of theophylline on its reaction with $^{\bullet}$OH.

Organic & Bimolecular Chemistry RSCPublishing

ARTICLE

3.4.1. Hydroxylation

The primary transformation product of the reaction of $^{\bullet}OH$ with theophylline, irrespective of reaction conditions, is 1, 3-dimethyluric acid (**i**). That is the one corresponding to hydroxylation of the parent molecule at carbon 8. The nearly diffusion controlled bimolecular rate constant (k_2 = (8.22 ± 0.03) × 10^9 dm^3 mol^{-1} s^{-1}) corresponding to the reaction of theophylline with $^{\bullet}OH$ determined during the pulse radiolysis studies is in accordance with the hydroxylation possibility (section 3.3.1). Previous studies on structurally similar molecules, such as caffeine and guanine, also pointed out a similar protocol.[9, 15, 43]

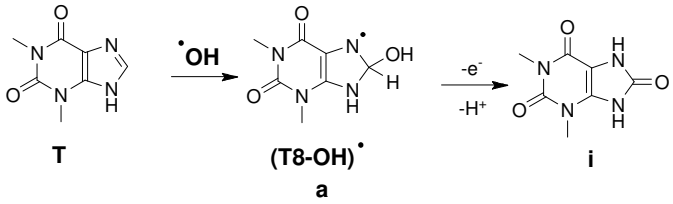

Scheme 3. Mechanism of the formation of 1,3-dimethyluric acid from theophylline.

The mechanism of the formation of this compound involves one electron oxidation of the early intermediate (T8-OH)$^{\bullet}$ followed by deprotonation (scheme 3). The OH radical adduct of guanine also undergoes an analogous mechanism that leads to the formation of 8-oxo-G,[49] a widely used biomarker for the oxidative stress.[9, 15]

3.4.2. Demethylation

Products corresponding to demethylation of methyl side chains of theophylline, that is 1 and 3-methylxanthine (**ii** and **iii**, both having M.W. 166.14 but different fragmentation pattern, figure S1 and S2, Supplementary information), is an important minor products in this reaction. This transformation is of biological relevance because of the potent anti-oxidant activities of methylxanthines.[36] Two distinct mechanisms viz. hydrogen abstraction and one electron oxidation are proposed as the gateway of demethylation.[36,50] To account the contribution of one electron oxidation in this process, end product studies were carried out in photo-irradiated samples of theophylline (1×10^{-4} mol dm^{-3}) in presence of 1×10^{-3} mol dm^{-3} $K_2S_2O_8$. Sulfate radical anion ($SO_4^{\bullet -}$), a specific one electron oxidant, is the reacting species in this case[45]. If one electron oxidation is the fundamental mechanism, ii and iii are expected in the end product profile. However, the targeted MS/MS analysis using LC-Q-TOF-MS did not give any information towards the formation of **ii** and **iii**. The involvement of one electron oxidation is thus eliminated from this case. Remaining possibility is the hydrogen abstraction. A multi-step mechanism is proposed by Santos and co-workers for this conversion.[36] The first step of the mechanism involves the hydrogen abstraction from one of the methyl side chain (for example: N_3-CH_3 in scheme 4) to form a carbon cantered radical (**b**). An instant electron release from radical b followed by hydrolysis generates a hydroxymethyl intermediate compound. The liberation of hydroxymethyl groups from this intermediate result the corresponding demethylated compound (**ii**).

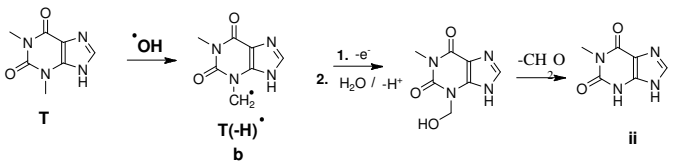

Scheme 4. Mechanism of the formation of 1-methylxanthine from theophylline.

3.4.3. Other products

The products **iv** – **xiv**, generated by the further conversion of the initial products by reactive species, were detected as minor peaks in the TIC. The mechanism of the isomeric uric acids (**iv** and **v**) are explained by two distinct mechanisms. First one is a hydroxylation-demethylation protocol in which the demethylation of **i**, formed as a result of hydroxylation of theophylline at carbon 8 (see scheme 2), at N_1 and N_3-CH_3 groups respectively results **iv** and **v**. Alternately, a demethylation-hydroxylation protocol is also possible in which hydroxylation of ii and iii at carbon 8 results the corresponding products. Likewise, demethylation of ii and iii results xanthine (**vi**) (Scheme 5).

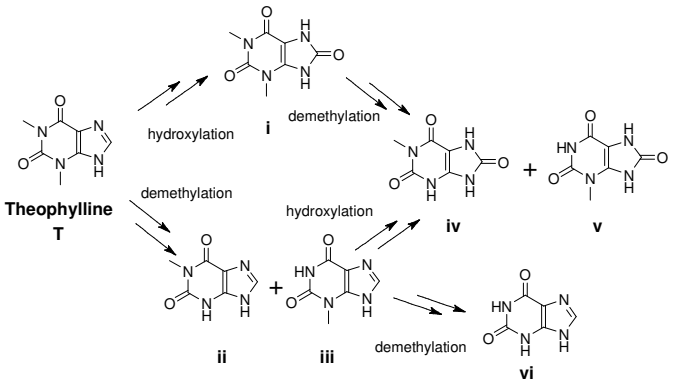

Scheme 5. Formation of xanthine and methyluric acids from theophylline.

As the photo-irradiation proceeds, the concentrations of some of the transformation products such as **i** could be equal (or even exceeds) to that of the parent compound. Hence the probability of $^{\bullet}OH$ attacks on the initially formed products rises. Similar observations were previously reported in the case of many organic compounds.[5, 6, 17]

The opening of the imidazole ring of (T8-OH)$^{\bullet}$ is presumed to be responsible for the formation of compounds **ix**-**xiv**. Analogues reactions are well explained in the case of hydroxyl radical adduct of guanine derivatives that leads to the formation of products such as FapyG.[9, 10, 15] However, compounds like vii

and viii, detected in extremely trace level, are not usually found in oxidative conditions. The mechanism corresponding to the formation of such products, observed in reducing conditions, in the present case is not clear. The possible side-reactions associated with H_2O_2 or the direct photo reduction of some of the initially formed products of theophylline (such as **ii**-**v**) by UV radiation is a likely reason for this conversion. The photo-transformation of aldehydes and ketones to corresponding alcohols are familiar in synthetic chemistry.[51] Moreover, the high sensitivity of LC-Q-TOF-MS allows the detection of such minor products without compromising the mass accuracy.

It is worth noting that, nearly 20% reduction in the photo degradation efficiency (at 6 min) is observed in the case of H_2O_2/photolysis in N_2 purged (that is deaerated) medium (Figure S21, Supplementary information). The high reactivity of $(A8\text{-}OH)^\bullet$ of N_6,N_6-dimethyladenosine against molecular oxygen is well renowned.[52] A likely reason for the enhanced degradation efficiency in aerated medium is the involvement of molecular oxygen in the reaction mechanism. This result is especially important because of the presence of molecular oxygen in most of the biological and environmental systems in which reactions of $^\bullet$OH occurs. Conversely, the concentration of the major oxidation product, 1,3-dimethyluric acid, formed in the case of N_2 purged condition was significantly higher. It is thus presumed that the presence of molecular oxygen in the medium induces further oxidation of the initially formed products like 1,3-dimethyluric acid.

4. Conclusions

The kinetic and mechanistic aspects of a representative methylxanthine drug, theophylline, against hydroxyl radical ($^\bullet$OH) have been explicated by pulse radiolysis and LC-Q-TOF-MS techniques. Two pathways - addition and hydrogen abstraction - are demonstrated for the reaction of $^\bullet$OH. The adduct radical $(T8\text{-}OH)^\bullet$ undergoes a ring opening reaction and yields products analogues to FapyG (a potential biomarker for the oxidative stress). LC-Q-TOF-MS analysis undoubtedly demonstrates the role of hydrogen abstraction also in the initial step of this reaction. This result is rather uncommon as $^\bullet$OH generally undergoes addition reaction with similar compounds. Characterization of various transformation products including isomeric xanthines (**ii** & **iii**) and uric acids (**iv** & **v**) by LC-Q-TOF-MS is an important illustration which is generally difficult to achieve. The rapid destruction of theophylline by H_2O_2/UV photolysis is an excellent hint of the vulnerability of this compound against oxidizing radicals. This is an important finding in the context of oxidation technologies for pollutant degradation. However, the efficiency of oxidizing radicals against the complete destruction of the parent as well as the transformed organic compound in natural waters could possibly be reduced due to scavenging of $^\bullet$OH by a variety of inorganic ions and dissolved organic matter. Therefore, additional efforts for assessing the efficiency and toxicity/TOC decline are essential for the practical implementation of these types of methodologies and are presently in progress.

5. Acknowledgements

We acknowledge National Centre for Free Radical Research, University of Pune, Pune for the pulse radiolysis facility. This work was performed under collaborative research scheme (Ref No. UGC-DAE-CSR-KC/CRS/09/RC02/1455) of UGC-DAE Consortium for Scientific Research, Kolkata Centre, Kolkata. CTA is thankful to DST (under PURSE and FIST scheme) for partial financial support. GP is thankful to SB College, Changanasserry for research guideship.

Notes and references

[a]School of Environmental Sciences, Mahatma Gandhi University, Kottayam.
[b]Advanced Centre of Environmental Studies and Sustainable Development, Mahatma Gandhi University, Kottayam.
[c]Department of Chemistry, N.S.S. Hindu College, Changanachery, India.
[c]UGC-DAE Consortium for Scientific Research, Kolkata Centre, Kolkata.
[c]Inter University Instrumentation Centre, Mahatma Gandhi University, Kottayam.

Electronic Supplementary Information (ESI) available: The spectral and kinetic parameters of the reaction of $^\bullet$OH, $SO_4^{\bullet-}$, $N_3^\bullet$ and $O^{\bullet-}$ with theophylline (table S1); MS and MS/MS spectra of selected transformation products (figure S1-S16); Decay (320 nm, 350 nm) traces in the case of reaction of $O^{\bullet-}$ (figure S17); Transient absorption spectrum of theophylline during its reaction with $SO_4^{\bullet-}$ and $N_3^\bullet$ at higher time scale (figure S18); UV-Vis Spectrum of theophylline at pH 6.0 and 10.1 (figure S19); Plot of absorbance of transient at 330 nm obtained by the reaction of theophylline with $^\bullet$OH against pH (figure S20); Percentage degradation of theophylline in N_2 purged and aerated conditions as a function of time (figure S21).. See DOI: 10.1039/b000000x/

1 E. Brillas, I. Sirés and M. A. Oturan, *Chemical Reviews*, 2009, **109**, 6570-6631.
2. P. Calza, C. Medana, E. Raso, V. Giancotti and C. Minero, *Rapid Communications in Mass Spectrometry*, 2011, **25**, 2923-2932.
3. J. De Laat, H. Gallard, S. Ancelin and B. Legube, *Chemosphere*, 1999, **39**, 2693-2706.
4. U. Kalsoom, S. S. Ashraf, M. A. Meetani, M. A. Rauf and H. N. Bhatti, *Chemical Engineering Journal*, 2012, **200–202**, 373-379.
5. R. Sreekanth, K. P. Prasanthkumar, M. M. Sunil Paul, U. K. Aravind and C. T. Aravindakumar, *The Journal of Physical Chemistry A*, 2013, **117**, 11261-11270.
6. M. M. Sunil Paul, U. K. Aravind, G. Pramod and C. T. Aravindakumar, *Chemosphere*, 2013, **91**, 295-301.
7. D. C. McDowell, M. M. Huber, M. Wagner, U. von Gunten and T. A. Ternes, *Environmental Science & Technology*, 2005, **39**, 8014-8022.
8. J. Cadet, T. Douki and J. L. Ravanat, *Free Radic Biol Med.*, 2010, **49**, 9-21.
9. C. Chatgilialoglu, M. D'Angelantonio, G. Kciuk and K. Bobrowski, *Chemical Research in Toxicology*, 2011, **24**, 2200-2206.
10. C. Chatgilialoglu, M. D'Angelantonio, M. Guerra, P. Kaloudis and Q. G. Mulazzani, *Angewandte Chemie International Edition*, 2009, **48**, 2214-2217.
11. A. Kumar, V. Pottiboyina and M. D. Sevilla, *The Journal of Physical Chemistry B*, 2011, **115**, 15129-15137.
12. T. L. Luke, T. A. Jacob, H. Mohan, H. Destaillats, V. M. Manoj, P. Manoj, J. P. Mittal, M. R. Hoffmann and C. T. Aravindakumar, *The Journal of Physical Chemistry A*, 2002, **106**, 2497-2504.
13. V. M. Manoj and C. T. Aravindakumar, *Chem. Commun.*, 2000, 2361-2362.

14. P. O'Neill, *Radiat Res*., 1983, **96**, 198-210.
15. S. Steenken, *Chemical Reviews*, 1989, **89**, 503-520.
16. J. A. Theruvathu, C. T. Aravindakumar, R. Flyunt, J. von Sonntag and C. von Sonntag, *Journal of the American Chemical Society*, 2001, **123**, 9007-9014.
17. S. P. Mezyk, T. J. Neubauer, W. J. Cooper and J. R. Peller, *The Journal of Physical Chemistry A*, 2007, **111**, 9019-9024.
18. W. Song, W. J. Cooper, S. P. Mezyk, J. Greaves and B. M. Peake, *Environmental Science & Technology*, 2008, **42**, 1256-1261.
19. K. Kummerer, *Chemosphere*, 2009, **75**, 417-434.
20. T. Heberer, *Toxicology Letters*, 2002, **131**, 5-17.
21. A. J. Ramirez, R. A. Brain, S. Usenko, M. A. Mottaleb, J. G. O'Donnell, L. L. Stahl, J. B. Wathen, B. D. Snyder, J. L. Pitt, P. Perez-Hurtado, L. L. Dobbins, B. W. Brooks and C. K. Chambliss, *Environmental Toxicology and Chemistry*, 2009, **28**, 2587-2597.
22. Y. Vystavna, F. Huneau, V. Grynenko, Y. Vergeles, H. Celle-Jeanton, N. Tapie, H. Budzinski and P. Le Coustumer, *Water Air Soil Pollut*, 2012, **223**, 2111-2124.
23. G. V. Buxton, C. L. Greenstock, W. P. Helman and A. B. Ross, Journal of Physical and Chemical Reference Data, 1988, **17**, 513-886.
24. L. P. Candeias and S. Steenken, Chemistry – *A European Journal*, 2000, **6**, 475-484.
25. A. J. Szentmiklosi, A. Cseppento, R. Gesztelyi, J. Zsuga, A. Kortvely, G. Harmati and P. P. Nanasi, *Current Medicinal Chemistry*, 2011, **18**, 3695-3706.
26. I. I. Koleva, T. A. van Beek, A. E. M. F. Soffers, B. Dusemund and I. M. C. M. Rietjens, *Molecular Nutrition & Food Research*, 2012, **56**, 30-52.
27. B. Stavric, *Food and Chemical Toxicology*, 1988, **26**, 541-565.
28. J. R. León-Carmona and A. Galano, International *Journal of Quantum Chemistry*, 2012, **112**, 3472-3478.
29. I. Baranowska, Kapinos, J, *CHEMIA ANALITYCZNA*, 2000, **45**, 53-58.
30. B. G. Cosio, A. Iglesias, A. Rios, A. Noguera, E. Sala, K. Ito, P. J. Barnes and A. Agusti, *Thorax*, 2009, **64**, 424-429.
31. K. V. Blake, K. L. Massey, L. Hendeles, D. Nickerson and A. Neims, *Annals of Emergency Medicine*, 1988, **17**, 1024-1028.
32. I. Kupsáková, A. Rybár, P. Dočolomanský, Z. Drobná, U. Stein, W. Walther, M. Barančík and A. Breier, *European Journal of Pharmaceutical Sciences*, 2004, **21**, 283-293.
33. H. Yin, X. Meng, H. Su, M. Xu and S. Ai, *Food Chemistry*, 2012, **134**, 1225-1230.
34. T. Antoniou, T. Gomes, M. Mamdani and D. Juurlink, *European Journal of Clinical Pharmacology*, 2011, **67**, 521-526.
35. R. Liang, A. Hu, W. Li and Y. N. Zhou, *Journal of Nanoparticle Research*, 2013, **15**, 1-13.
36. P. Santos, S. Silva, G. Justino and A. Vieira, *Redox Report*, 2010, **15**, 138-144.
37. G. V. Buxton and C. R. Stuart, *Journal of the Chemical Society, Faraday Transactions*, 1995, **91**, 279-281.
38. K. M. S. Yadav P, Shirdhonkar M. B, Rao B.S. M, *Curr. Sci*, 2007, **92**, 599-605.
39. C. L. Yu, T. M. Louie, R. Summers, Y. Kale, S. Gopishetty and M. Subramanian, *J Bacteriol*., 2009, **191**, 4624-4632.
40. P. Manoj, H. Mohan, J. P. Mittal, V. M. Manoj and C. T. Aravindakumar, *Chemical Physics*, 2007, **331**, 351-358.
41. D. B. Naik and K. Kishore, *Research on Chemical Intermediates*, 2002, **28**, 603-617.
42. T. L. Luke, H. Mohan, V. M. Manoj, P. Manoj, J. P. Mittal and C. T. Aravindakumar, *Research on Chemical Intermediates*, 2003, **29**, 379-391.
43. J. P. Telo and A. J. S. C. Vieira, *Journal of the Chemical Society, Perkin Transactions* 2, **1997**, 1755-1758.
44. K. Kobayashi and S. Tagawa, *Journal of the American Chemical Society*, 2003, **125**, 10213-10218.
45. P. Neta, R. E. Huie and A. B. Ross, *Journal of Physical and Chemical Reference Data*, 1988, **17**, 1027-1284.
46. P. M. P. Santos, J. P. Telo and A. J. S. C. Vieira, *Redox Report*, 2008, **13**, 123-133.
47. E. Cavalieri and E. Rogan, *Environmental Health Perspectives*, 1985, **64**, 69-84.
48. A. F. Lehner, J. Horn and J. W. Flesher, *Biochemical and Biophysical Research Communications*, 2004, **322**, 1018-1023.
49. L. I. Shukla, A. Adhikary, R. Pazdro, D. Becker and M. D. Sevilla, *Nucleic Acids Research*, 2004, **32**, 6565-6574.
50. P. M. P. Santos, A. M. M. Antunes, J. Noronha, E. Fernandes and A. J. S. C. Vieira, *European Journal of Medicinal Chemistry*, 2010, **45**, 2258-2264.
51. N. Kambe, K. Kondo, S. Murai and N. Sonoda, *Angewandte Chemie International Edition in English*, 1980, **19**, 1008-1009.
52. A. J. S. C. Vieira and S. Steenken, *Journal of the American Chemical Society*, 1987, **109**, 7441-7448.

